

Hyper viscosity and vorticity-based models for subgrid scale modeling

G. Dantinne, H. Jeanmart, G.S. Winckelmans and V. Legat
*Center for Systems Engineering and Applied Mechanics,
Université catholique de Louvain, 1348 Louvain-la-Neuve, Belgium*

D. Carati
*Service de Physique Statistique, Plasma et Optique Non Linéaire, CP231
Université Libre de Bruxelles, Campus Plaine, 1050 Brussels, Belgium*

20 November 1997

Abstract. Large-eddy simulations corresponding to the decaying isotropic turbulence experiment of Comte-Bellot and Corrsin are performed, using a pseudo-spectral code that incorporates four models: viscosity and hyper viscosity types, each implemented for both the subgrid scale stress tensor and the subgrid scale force. Two $1/T$ scalings are also considered for the viscosity amplitude. The dynamic procedure is extended to the four models and is tested. Results are obtained with and without this procedure and for both scalings. The main conclusions are: (a) the two viscosity models perform equally well; (b) the Kolmogorov scaling performs as well as the Smagorinsky scaling, yet it is computationally more efficient; (c) in the dynamic procedure, there is a fairly wide range of test to grid filter ratios which produces results insensitive to this ratio; (d) the hyper viscosity models lead to energy decay curves that follow the experimental data as well as the usual viscosity models.

Key words: Turbulence, simulation, modeling.

Abbreviations: LES – large eddy simulation; sgs – subgrid scale; DNS – direct numerical simulation

1. Formulation

When a filter (hereafter denoted $\overline{\cdot\cdot}$) is applied to the Navier-Stokes equations for incompressible flow, an unknown sgs stress $\tau_{ij} = \overline{u_i u_j} - \overline{u_i} \overline{u_j}$ appears in the resulting LES equations. Classically, the sgs tensor has been modeled in terms of the velocity gradient. More precisely, the traceless part, τ_{ij}^* ,¹ has been modeled in terms of the resolved strain rate tensor $\overline{S}_{ij} = (\partial_j \overline{u_i} + \partial_i \overline{u_j})/2$. The trace can be lumped into the ‘pressure’, by defining $\overline{P}^* = \overline{P} + \frac{1}{3} \tau_{kk}$, and does not affect the flow dynamics. Such a formulation has been popularized by Smagorinsky [1] who proposed an eddy viscosity model for the sgs stress tensor with an eddy viscosity scaled with the filter width and the local strain amplitude.

¹ The superscript “*” will always denote the traceless part of a tensor in the following. When appearing in a vector, this superscript means that the vector is the divergence of a traceless tensor.

The main advantages of the Smagorinsky model are its simplicity and its stability. It is well-known that, when the Smagorinsky model is compared to the actual sgs stress that can be computed from DNS, very poor correlation coefficients are measured (see, e.g., [2, 3]). Moreover, the Smagorinsky model is purely dissipative while it is usually admitted that the small scales may locally play the role of a source of energy for the resolved scales [4, 5, 6]. Hence, although it is sometimes argued that the only relevant task of a sgs model is to dissipate the correct amount of energy in average, there are some important motivations for exploring new sgs models [3, 7, 8].

Before presenting these new models, we first stress that only the sgs force, $f_i^* = \partial_j \tau_{ij}^*$, appears in the Navier-Stokes equation and hence really needs to be modeled. Moreover, only the solenoidal part of that force, g_i^* , affects the flow dynamics[3]. The difference between f_i^* and g_i^* is the gradient of a scalar ϕ , and hence it can also be lumped into the ‘pressure’ by defining $\overline{\mathcal{P}}^* = \overline{P}^* + \phi$.

The purpose of this work is to investigate different simple possibilities for the modeling of the sgs stress tensor, τ_{ij}^* , or the sgs forcing, g_i^* . We present in Table I the different models that have been considered in this work[3].

Table I. Subgrid scale models.

Model	formulation
1	$\tau_{ij}^* = -2 \nu_t \overline{S}_{ij}$
2	$\tau_{ij}^* = 2 \overline{\Delta}^2 \nu_t \nabla^2 \overline{S}_{ij}$
3	$g_i^* = \epsilon_{imn} \partial_m (\nu_t \overline{\omega}_n)$
4	$g_i^* = -\overline{\Delta}^2 \epsilon_{imn} \partial_m (\nu_t \nabla^2 \overline{\omega}_n)$

where ∇^2 stands for the Laplacian operator and ϵ_{ijk} is the fully anti-symmetric rank 3 tensor with $\epsilon_{123} = 1$. The length scale $\overline{\Delta}$ corresponds to the filter width. Summation over repeated indices is assumed. Clearly, the parameter ν_t has the same dimension as a viscosity. However, the physical meaning of this quantity depends on the model. It can be understood as an eddy viscosity in models 1 and 3 while the product $\overline{\Delta}^2 \nu_t$ plays the role of an hyper eddy viscosity in models 2 and 4. Two different scalings for ν_t have been considered. They are presented in Table II.

Table II. Eddy viscosity scaling.

Model	Formulation
Smagorinsky <i>a</i>	$\nu_t = C \overline{\Delta}^2 \overline{S} $
Kolmogorov <i>b</i>	$\nu_t = C_K \overline{\Delta}^{4/3} \overline{\epsilon}^{1/3}$

where C and C_K are dimensionless constants and $|\overline{S}| = (2\overline{S}_{ij}\overline{S}_{ij})^{1/2}$. The scaling *b* follows the Kolmogorov[11] dimensional analysis. It uses the filter width $\overline{\Delta}$ as the length scale and $(\overline{\Delta}^2/\overline{\epsilon})^{1/3}$ as the time scale. Here, $\overline{\epsilon}$ represents the rate of energy transfer within the inertial range (assumed constant). In a LES, the use of the Kolmogorov scaling implicitly assumes that the quantity $\overline{\epsilon}$ is accessible during the simulation. Usually, this is not the case and this has motivated alternative scaling like *a* in which $\overline{\epsilon}$ is approximated by invoking local equilibrium between the rate of energy transfer within the inertial range and the subgrid scale dissipation $\overline{\epsilon} \approx -\tau_{ij}^* \overline{S}_{ij}$. This yields the classical Smagorinsky scaling *a* for the eddy viscosity. The following relation between C and C_K can also be derived:

$$C \approx C_K^{3/2}. \quad (1)$$

However, it has been shown that the local equilibrium approximation is not required when the dynamic procedure is used [9, 10]. In that context, the Kolmogorov scaling has the practical advantage that (i) it is simpler, and (ii) fewer filtering operations are required when implementing the dynamic procedure.

The dynamic procedure is based on the application of an additional test filter to the LES equations. This test filter is usually denoted by $\widehat{\cdot}$ and is characterized by a filter width $\widehat{\Delta} > \overline{\Delta}$. It generates another sgs tensor corresponding to a coarser resolution $T_{ij}^* = (\widehat{u}_i \widehat{u}_j - \widehat{u}_i \widehat{u}_j)^*$. The comparison between the different stress tensors leads to the Germano identity [12]

$$L_{ij}^* + \widehat{\tau}_{ij}^* - T_{ij}^* = 0, \quad (2)$$

where $L_{ij}^* = (\widehat{u}_i \widehat{u}_j - \widehat{u}_i \widehat{u}_j)^*$ is known in terms of the resolved velocity field. The modeling of the subgrid scale tensors violates the identity (2). For the Smagorinsky model, the dynamic procedure [13, 14, 15, 16, 17] is implemented by assuming that (i) the same type of model can be used for τ_{ij}^* and T_{ij}^* , (ii) the same value of the dimensionless parameter C can be used in τ_{ij}^* and T_{ij}^* , (iii) for homogeneous flow, the situation considered here, C is independent of position, (iv) C is correctly approximated by a global least square minimization of the left hand side of Eq.(2). For scaling *b*, the same assumptions are made for the *dimensional product* $\check{C} = C_K \overline{\epsilon}^{1/3}$. This is justified if both filters

lie in the inertial range so that $\bar{\tau}$ is indeed the same at both filter sizes. The dynamic procedure leads, for models 1 and 2, to:

$$C = \frac{\langle \gamma_{ij}^* L_{ij}^* \rangle}{\langle \gamma_{ij}^* \gamma_{ij}^* \rangle}, \quad \tilde{C} = \frac{\langle \tilde{\gamma}_{ij}^* L_{ij}^* \rangle}{\langle \tilde{\gamma}_{ij}^* \tilde{\gamma}_{ij}^* \rangle}, \quad (3)$$

where $\langle \dots \rangle$ denotes the volume averaging and

$$\gamma_{ij}^*(1-a) = 2 \left[\overline{\Delta^2} |\widehat{S}| \widehat{S}_{ij} - \widehat{\Delta}^2 |\widehat{S}| \widehat{S}_{ij} \right], \quad (4a)$$

$$\tilde{\gamma}_{ij}^*(1-b) = 2 \left[\overline{\Delta^{4/3}} - \widehat{\Delta}^{4/3} \right] \widehat{S}_{ij}, \quad (4b)$$

$$\gamma_{ij}^*(2-a) = -2 \left[\overline{\Delta^4} |\widehat{S}| \widehat{\nabla^2 S}_{ij} - \widehat{\Delta}^4 |\widehat{S}| \widehat{\nabla^2 S}_{ij} \right], \quad (4c)$$

$$\tilde{\gamma}_{ij}^*(2-b) = -2 \left[\overline{\Delta^{10/3}} - \widehat{\Delta}^{10/3} \right] \widehat{\nabla^2 S}_{ij}. \quad (4d)$$

We see that the procedure for scaling b is indeed computationally more efficient than what is obtained when using scaling a . For isotropic turbulence, one obtains that $\tilde{C} = \tilde{C}(t)$ and $C = C(t)$. Hence, the Kolmogorov scaling b produces a uniform eddy viscosity, $\nu_t(t)$. Because of the spatial variations of $|\widehat{S}|$, this is not the case when using the Smagorinsky scaling a .

Notice that model 3 only differs from the classical Smagorinsky model by terms proportional to the spatial derivatives of ν_t . Hence, for isotropic turbulence and scaling b (which lead to $\nu_t = \nu_t(t)$), the models are identical: 1- $b \equiv 3$ - b . Other types of models that would not be purely dissipative can be constructed as well [3, 6, 7]. They are not considered in the present paper. The dynamic procedure can be extended to models 3 and 4 for the sgs force. In that case, one obtains

$$C = \frac{\langle \gamma_i^* l_i^* \rangle}{\langle \gamma_i^* \gamma_i^* \rangle}, \quad \tilde{C} = \frac{\langle \tilde{\gamma}_i^* l_i^* \rangle}{\langle \tilde{\gamma}_i^* \tilde{\gamma}_i^* \rangle}, \quad (5)$$

where $l_i^* = \partial_j L_{ij}^*$ and

$$\gamma_i^*(3-a) = -\epsilon_{imn} \partial_m \left[\overline{\Delta^2} |\widehat{S}| \widehat{\omega}_n - \widehat{\Delta}^2 |\widehat{S}| \widehat{\omega}_n \right] \quad (6a)$$

$$\begin{aligned} \tilde{\gamma}_i^*(3-b) &= -\epsilon_{imn} \partial_m \left[\overline{\Delta^{4/3}} - \widehat{\Delta}^{4/3} \right] \widehat{\omega}_n \\ &= \left[\overline{\Delta^{4/3}} - \widehat{\Delta}^{4/3} \right] \nabla^2 \widehat{u}_i \end{aligned} \quad (6b)$$

$$\gamma_i^*(4-a) = \epsilon_{imn} \partial_m \left[\overline{\Delta^4} |\widehat{S}| \widehat{\nabla^2 \omega}_n - \widehat{\Delta}^4 |\widehat{S}| \widehat{\nabla^2 \omega}_n \right] \quad (6c)$$

$$\begin{aligned} \tilde{\gamma}_i^*(4-b) &= \epsilon_{imn} \partial_m \left[\overline{\Delta^{10/3}} - \widehat{\Delta}^{10/3} \right] \widehat{\nabla^2 \omega}_n \\ &= - \left[\overline{\Delta^{10/3}} - \widehat{\Delta}^{10/3} \right] \nabla^2 \widehat{u}_i. \end{aligned} \quad (6d)$$

2. Results

In this section, we present results obtained using the above models for LES of decaying isotropic turbulence, with comparison to the experiment of Comte-Bellot and Corrsin [18].

In order to carry out the LES's, a pseudo-spectral code with a '3/2 dealiasing rule' has been developed. The LES equations are integrated in time using a third order Runge-Kutta scheme for the non linear terms and an analytical integration for the viscous terms. The time step is 10^{-3} s and the eddy viscosity is computed only once per time step.

The initial velocity field is generated by choosing the amplitudes of the Fourier modes so as to match the 3-D energy spectrum to that measured experimentally at the first station (see [19]). The phases are chosen randomly. These non-physical initial conditions are then 'relaxed' by first letting the flow evolve for a few time steps (typically 10 to 50) and then by rescaling back the amplitudes to retrieve the initial spectrum. This procedure is repeated several times (typically 5 to 10 times). The obtained velocity field then contains more realistic phase information and can be used as a good initial condition.

Simulations were first carried out on a 32^3 grid for all four models, with scaling a , and using a constant value for C . The C -value was optimized so as to obtain the 'best' energy decay curve. The resulting evolution for the resolved energy (i.e., the fraction of the total energy that is resolved by the computation) is presented in Fig. 1. With our resolution, the initial resolved energy corresponds to 75% of the total energy. Consequently, the subgrid scales carry less energy than the resolved scales which is a basic requirement for LES.

As expected with C constant, models 1- a and 3- a on the one hand, 2- a and 4- a on the other hand, give essentially the same results. The viscosity models dissipate too much energy in the late stages of decay. The hyper viscosity models do not dissipate enough energy in the late stages. Increasing C in hyper viscosity models increases the dissipation in the early stages but it does not affect much the late stages. Obviously, viscosity and hyper viscosity models exhibit different behaviors (different curvatures) during the early stages.

The experimental and computed spectra at station 2 are shown in Fig. 2. It is seen that the models predict the spectrum reasonably well, except in the high wavenumber range. Notice that we could have optimized C so as to obtain better looking spectra at station 2, but this

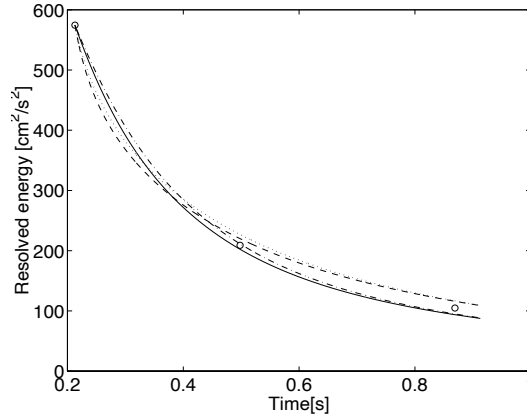


Figure 1. Evolution of the resolved energy for the four models with scaling a and with constant C . Solid curve: model 1 with $C = 0.019$, dashed-dotted curve: model 2 with $C = 0.01$, dashed curve: model 3 with $C = 0.019$, dotted curve: model 4 with $C = 0.01$, circles: experimental data.

would have resulted in an energy decay curve further away from the experimental data (especially for the hyper viscosity models).

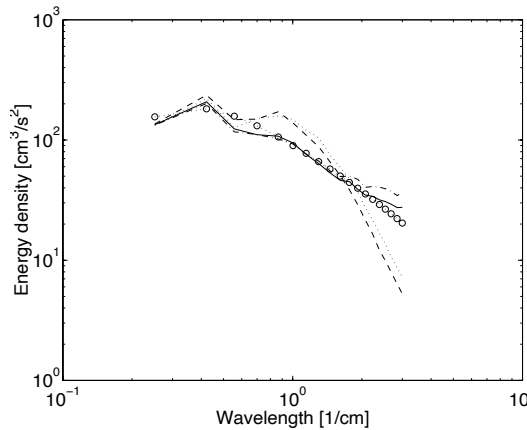


Figure 2. Resolved spectra corresponding to station 2. Solid curve: model 1 with $C = 0.019$, dashed-dotted curve: model 2 with $C = 0.01$, dashed curve: model 3 with $C = 0.019$, dotted curve: model 4 with $C = 0.01$, circles: experimental data.

The results for the energy decay are in fair agreement with the experiment. However, C was specified and kept constant. The dynamic procedure which produces the suitable $C(t)$ (or $C'(t)$) is now considered. The test and grid filters are sharp spectral cutoffs. Their width ratio, $\alpha = \hat{\Delta}/\bar{\Delta}$, is first taken as $\alpha = 2$.

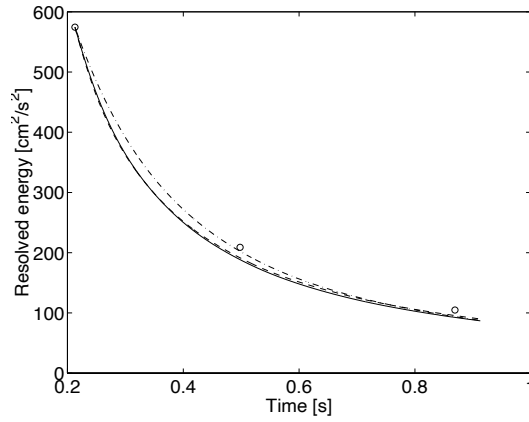


Figure 3a. Energy decay for models 1-*a* (dashed curve) and 1-*b* (solid curve). Decay for model 1-*a* with constant C (dashed-dotted curve) is also shown. Circles are experimental data.

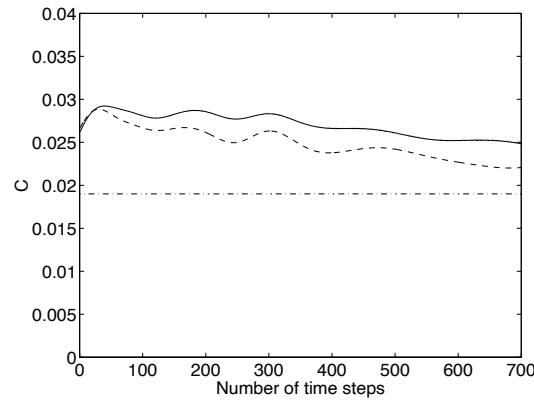


Figure 3b. Comparison of the C values for model 1, scalings *a* (dashed curve) and *b* (solid curve). Circles are experimental data.

At first, both the classical and the Kolmogorov scalings on the eddy viscosity model (1-*a* and 1-*b*) are considered. The results are shown in Fig. 3a. As expected, the two models with the dynamic procedure produce rather similar energy decays since they both are of the viscosity type. The obtained curvatures in the energy decay curves appear better than what is obtained with C constant, even if the dynamic procedure leads to a more dissipative behavior during the early stages.

Models 1-*a* and 1-*b* thus produce results that are of equivalent quality. This observation is strengthened if we consider the time evolution of the C value as presented in Fig. 3b. Notice that, for scaling *b*, the

C value reported in the figure is computed from Eq. 1 and the C' definition. The mean dissipation rate, $\bar{\epsilon}$, is estimated through numerical time differentiation of the resolved energy curve.

The C values obtained with both scalings are not expected to be the same. Indeed, while the Smagorinsky scaling is based on a local equilibrium hypothesis, the Kolmogorov scaling relies on the mean dissipation rate.

Since the Kolmogorov scaling requires substantially fewer filtering operations than the Smagorinsky scaling [10], it is used for all following simulations.

The energy decay obtained with all four models and with the dynamic procedure is shown in Fig. 4. These computations were carried out using the same grid and filters as before. It is seen that models 1- b and 3- b are slightly too dissipative and that models 2- b and 4- b are not dissipative enough.

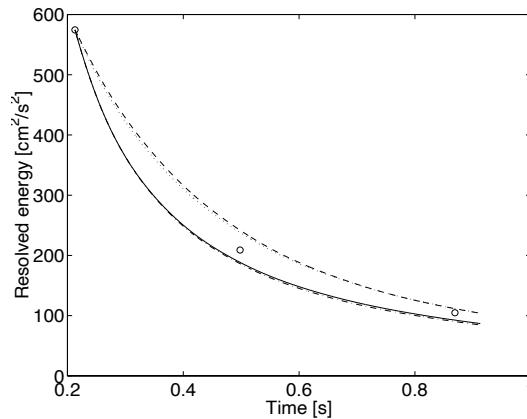


Figure 4. Resolved energy decay for all models with scaling b . Solid curve: model 1, dashed-dotted curve: model 2, dashed curve: model 3, dotted curve: model 4, circles: experimental data.

Hyper viscosity models appear to provide an energy decay curve ‘as good’ as the one obtained with classical eddy viscosity models. This partly supports some of the hopes formulated for these models after performing *a priori* tests on DNS databases [3]. These models certainly deserve further investigations.

Furthermore, it has been observed that the ratio, α , between the filter widths could affect strongly C (or C') and thus the energy decay rate. For each model, it appears that there exists a rather large range of ratios producing similar decay curves. Outside this range, the results become highly dependent on the value of α .

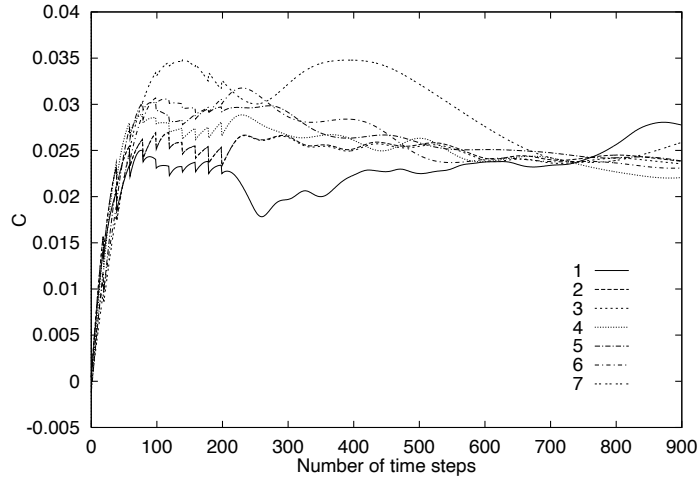


Figure 5a. Influence of α on C for model 1-a. The first 200 time steps correspond to the setting of realistic initial conditions. 1: $\alpha = 1.1$, 2: $\alpha = 1.2$, 3: $\alpha = 1.5$, 4: $\alpha = 2.0$, 5: $\alpha = 2.5$, 6: $\alpha = 3.0$, 7: $\alpha = 4.0$

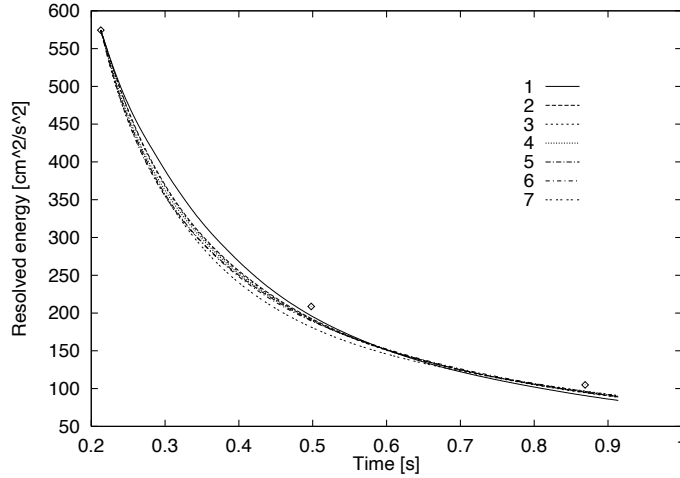


Figure 5b. Influence of α on the resolved energy decay for model 1-a. 1: $\alpha = 1.1$, 2: $\alpha = 1.2$, 3: $\alpha = 1.5$, 4: $\alpha = 2.0$, 5: $\alpha = 2.5$, 6: $\alpha = 3.0$, 7: $\alpha = 4.0$, circles = experimental data

For instance, Figs. 5a and 5b show the influence of α on the computed C and on the resolved energy decay for model 1-a. The various curves correspond to a fixed effective grid filter, $\bar{\Delta}$, and to different test filters, $\hat{\Delta}$.

Similar behaviors have been observed for all models and both scalings. However, the range of α seems to depend on the model. If we compare viscosity models, we observe that the ranges for the models 1-*b* and 3-*b* are slightly different. Recall that, since $\nu_t = \nu_t(t)$ only, these models are equivalent. However, the dynamic procedure for 3-*b* is different from that used for 1-*b*. In the first case, C is determined by optimization at the sgs stress tensor level while it is obtained from an optimization at the sgs force vector level in the second case.

3. Conclusion

Large eddy simulations of the decaying isotropic turbulence experiment of Comte-Bellot and Corrsin have been performed, using a pseudo-spectral code that incorporates some subgrid scale models proposed in [3]. More specifically, eddy viscosity and hyper eddy viscosity models have been considered for this paper. For each model class, two formulations have been tested: the classical formulation based on strain rate and a vorticity-based formulation. This leads to four different ‘models’. For each model, two scalings for the eddy viscosity have been considered: the classical Smagorinsky scaling and the ‘Kolmogorov’ scaling proposed in [10]. The dynamic procedure has been extended to all four models and to both scalings, and has been tested numerically. Results have been obtained with and without the dynamic procedure and have been compared.

One conclusion of this investigation is that the Kolmogorov scaling produces results in the dynamic procedure that are very similar to those obtained with the classical Smagorinsky scaling. Yet, it is computationally much more efficient because fewer filtering operations are required.

Another conclusion is that hyper viscosity models produce an energy decay curve that follows the experimental data for the whole time period covered by the experiment as well as the usual eddy viscosity models. This result is also supported by *a priori* tests performed on a 512^3 DNS database of the same experiment [3]: higher correlations with the actual sgs stress tensor and sgs solenoidal forcing were indeed obtained. Hyper viscosity LES models deserve further investigations.

Finally, the influence of the ratio between the two filter widths used in the dynamic procedure has been probed numerically. It has been found that there is a wide range of ratios leading to essentially the same decay curves. This range depends on the models and on the scalings. This sensitivity is most likely related to the higher order derivatives required in the dynamic procedure.

One of the future aims of our work is to test some LES models in the vorticity-velocity formulation of the Navier-Stokes equation [3] instead of the present velocity-pressure formulation. Indeed, *a priori* tests have shown that the correlations between the modeled and actual sgs terms are higher in vorticity-velocity LES than in velocity-pressure LES. In vorticity-velocity LES, models based on the resolved vorticity appear as natural candidates. This is confirmed by preliminary results.

Acknowledgments

G.D. has been supported by a grant from the FRIA, Belgium. V.L. and D.C. are “Chercheurs Qualifiés du Fonds National pour la Recherche Scientifique”, Belgium.

References

1. Smagorinsky, J, General circulation experiments with the primitive equations, *Mon. Weath. Rev.* **93**, 99–165 (1963)
2. Clark, R. A., Ferziger, J. H. and Reynolds, W. C., Evaluation of subgrid-scale models using an accurately simulated turbulent flow, *J. Fluid Mech.* **91**, 1–16 (1979).
3. Winckelmans, G. S., Lund, T. S., Carati, D. & Wray A. A., A priori testing of subgrid-scale models for the velocity-pressure and vorticity-velocity formulations, *Summer Program*, Center for Turbulence Research (Stanford University and NASA Ames), 309–328 (1996).
4. Leith, C., Stochastic backscatter in a subgrid-scale model: Plane shear mixing layer, *Phys. Fluids A* **2**, 297–299 (1990).
5. Mason, P. and Thomson, D., Stochastic backscatter in large-eddy simulations of boundary layers, *J. Fluid Mech.* **242**, 51–78 (1992).
6. Carati, D., Ghosal, S. & Moin, P., On the representation of backscatter in dynamic localization models, *Phys. Fluids* **7**(3): 606–616 (1995).
7. Lund, T. S. & Novikov, E. A., Parametrization of subgrid-scale stress by the velocity gradient tensor, *Annu. Res. Briefs*, Center for Turbulence Research (Stanford University and NASA Ames), 27–43 (1992).
8. Meneveau, C. & Lund, T. S., Search for subgrid-scale parametrization by projection pursuit regression, *Summer Program*, Center for Turbulence Research (Stanford University and NASA Ames), 61–82 (1992).
9. Wong, V.C. and Lilly, D., A comparison of two subgrid closure methods for turbulent thermal convection, *Phys. Fluids* **6**, 1016–1023 (1994).
10. Carati, D., Jansen, K. & Lund, T., A family of dynamic models for large-eddy simulation, *Annu. Res. Briefs*, Center for Turbulence Research (Stanford University and NASA Ames), 35–40 (1995).
11. Kolmogorov, A.N., Local structure of turbulence in an incompressible fluid at very high Reynolds number, *Dokl. AN SSSR* **30**, 301, (1941).
12. M. Germano, Turbulence: the filtering approach, *J. Fluid Mech.* **238**, 325 (1992).
13. Germano, M., Piomelli, U., Moin, P. & Cabot, W., A dynamic subgrid-scale eddy-viscosity model, *Phys. Fluids A* **3**(7): 1760–65 (1991).

14. Ghosal, S., Lund, T. S. & Moin, P., A local dynamic model for large-eddy simulation, *Annu. Res. Briefs*, Center for Turbulence Research (Stanford University and NASA Ames), 3–25 (1992).
15. Ghosal, S., Lund, T. S., Moin, P. & Akselvoll, K., A dynamic localization model for large-eddy simulation of turbulent flows, *J. Fluid Mech.* 286: 229–255 (1995).
16. Moin, P. & Jimenez, J., Large eddy simulation of complex turbulent flows, *AIAA 24th Fluid Dynamics Conference*, Orlando, FL., AIAA paper 93-3099 (1993).
17. Moin, P., Carati, D., Lund, T., Ghosal, S. & Akselvoll, K., Developments and applications of dynamic models for large eddy simulation of complex flows, *74th Fluid Dynamics Symposium on Application of Direct and Large Eddy Simulation to Transition and Turbulence*, Chania, Crete, Greece, AGARD-CP-551, 1–9 (1994).
18. Comte-Bellot, G. & Corrsin, S., Simple Eulerian time-correlation full and narrow-band velocity signals in grid-generated ‘isotropic’ turbulence, *J. Fluid Mech.* 48: 273–337 (1971).
19. Rogallo R. S., Numerical experiments in homogeneous turbulence, *NASA technical Memorandum 81315* (1981).
20. Rogallo R. S. & Moin, P., Numerical simulation of turbulent flows, *Annu. Rev. Fluid Mech.* 16: 99–137 (1984).

Address for correspondence: G. Dantinne, CESAME (MEMA), Bâtiment Euler, Av. Lemaître, 4 Université catholique de Louvain, 1348 Louvain-la-Neuve, Belgium